ELSEVIER

Journal of Molecular Structure (Theochem) 588 (2002) 55–69

THEO CHEM

www.elsevier.com/locate/theochem

DFT calculations on the electronic and geometrical structure of 18-crown-6 complexes with Ag^+, Hg^{2+}, Ag^0, Hg^+, Hg^0, $AgNO_3$, and HgX_2 (X = Cl, Br, and I)

A.A. Bagatur'yants[a,*], A.Ya. Freidzon[a], M.V. Alfimov[a], E.J. Baerends[b], J.A.K. Howard[c], L.G. Kuz'mina[d]

[a]*Center of Photochemistry, Institute of Chemical Physics, Russian Academy of Sciences, ul. Novatorov 7a, Moscow 117421 Russian Federation*
[b]*Afdeling Theoretische Chemie, Vrije Universiteit, De Boelelaan 1083, 1081 HV Amsterdam, The Netherlands*
[c]*Department of Chemistry, University of Durham, Durham DH1 3LE, UK*
[d]*Kurnakov Institute of General and Inorganic Chemistry, Russian Academy of Sciences, Leninskii pr. 31, Moscow 117907 Russian Federation*

Received 2 January 2002; revised 12 March 2002; accepted 12 March 2002

Abstract

Density functional theory is used for molecular simulation of the electronic and geometrical structure of 18-crown-6, its complexes with Ag^+, Hg^{2+}, Ag^0, Hg^+, Hg^0, $AgNO_3$, and HgX_2 (X = Cl, Br, and I). Ab initio MP2/6-31G* calculations are performed for the two main conformations of the free crown ether and for anion-free complexes. The complex formation energies are analysed in terms of various contributions including Pauli and electrostatic repulsion and orbital interactions according to the Morokuma scheme. It is found that the Hg^{2+} ion is most strongly bound to the crown ether; silver and mercury ions in the 18-crown-6 cavity can capture an electron, and neutral 18-crown-6 complex of silver can be bound through van der Waals-type interactions. The stability of metal complexes with supporting anionic ligands is determined not only by the cation charge, but also by the type of the ligand.

Keywords: Density functional theory; Crown ethers; Silver; Mercury

1. Introduction

Crown ethers are widely used as complexing agents that can capture selectively metal cations in their cavity. Typical examples are provided by the use of crown ethers for extraction of heavy metals from aqueous solutions, separation of various metal cations, and stabilization of metal cations in organic media, and in crown ether-based sensors for these cations. Their ability to bind metal cations depends on the cavity size, the nature of heteroatoms (oxygen, nitrogen, or sulfur) and substituents in the macrocycle, and the solvent.

Recently, crown ethers have found new application as components of supramolecular systems [1]. A crown ether fragment with a metal cation captured in its cavity may serve in such systems as a structure-forming or switching unit. The coordination of a metal cation in the crown ether cavity or a change of its oxidation number may affect the properties of the functional fragment. These effects can be mediated either through the crown ether heteroatoms involved

* Corresponding author. Tel.: +7-95-936-2588; fax: +7-95-936-1255.
E-mail address: sasha@photonics.ru (A.A. Bagatur'yants).

0166-1280/02/$ - see front matter
PII: S0166-1280(02)00119-7

within the conjugated chain of the functional fragment or through binding sites of the functional fragment directly interacting with the metal cation. Thus, supramolecular structures that involve a crown ether fragment and a dye as a functional group were suggested as photoswitched molecular devices [2–4]. The effects of metal coordination on the photosensitive properties of crown ether complexes were studied, for example, in Refs. [2,5–9].

The change of the oxidation number of the metal ion coordinated inside the crown ether cavity through its chemical or photochemical reduction (or oxidation) can also be used in principle for creating switching or photoswitching supramolecular systems. It was reported [10–12] that silver(I) complexes with some diaza-18-crown-6 derivatives can be reduced in solution to a zero-charged complex with a neutral silver atom in the crown ether cavity. This result can be interpreted in the sense that a highly polarizable heavy metal cation in crown ether complexes can serve as an electron trap.

Thus, the interaction of heavy d-block metals with crown ethers and electronic properties of their crown ether complexes are of great interest for many practical reasons. Heavy d-block metals can specifically interact with various ligands and various binding sites. This property can be used for the directed design of various supramolecular metal–ligand structures. d-Block metals can exist in different oxidation states; thus, changing the oxidation state of the metal ion coordinated in the crown ether cavity may be used for controlling the structure and properties of supra and macromolecular systems (as in haemoglobin). Finally, heavy metals can participate in strong closed-shell interactions and, hence, can assist in assembling systems of complex molecular architecture (clusters, polynuclear complexes, etc.) [13].

Free crown ethers, protonated crown ethers, ammonium crown ether complexes, and crown ether complexes of alkali or alkaline-earth metals were rather extensively studied theoretically. In particular, ab initio studies of these systems at various theoretical levels were reported in many articles [14–21]. The structure and the binding energies of 18-crown-6 (18c6) complexes of alkali and alkaline-earth metals were calculated at the Hartree–Fock and MP2 levels in Refs. [14–16]. The K^+ complexes of 18-crown-6 and 12-crown-4 were investigated in Ref. [16] by ab initio (MP2 and MP4) and by density functional methods. Ab initio calculations were performed in hybrid 6-31 + G*, cc-pVxZ, and aug-cc-pVxZ basis sets with relativistic effective core potentials (ECPs) for metal ions [14–16]. The problem of alkali metal–crown ether interaction was further investigated in Refs. [17–20]. The proton affinities of various crown ethers were also examined at the MP2/6-31(+)G(**) level in Ref. [21].

However, no theoretical investigation has been reported so far on crown ether complexes of heavy metal cations. This may be explained by the difficulties associated with taking into account both electron correlation and relativistic effects, which are very important in the case of heavy metal systems.

This paper is devoted to a combined theoretical density functional theory (DFT) and ab initio study of the structure and relative stability of silver(I) and mercury(II) 18-crown-6 complexes. We also considered the structures of Ag^0, Hg^+, and Hg^0 complexes with 18-crown-6 in order to examine the reduction of these cations ($Ag^+ \rightarrow Ag^0$, $Hg^{2+} \rightarrow Hg^+ \rightarrow Hg^0$) in the crown ether cavity. Finally, we investigated the effect of counterions on the structure and relative stability of silver(I) and mercury(II) 18-crown-6 complexes. There are structural data published for a series of mercury halide 18-crown-6 complexes HgX_2:18c6 (X = Cl, Br, and I) [22–24], and we selected this series for a comparative theoretical investigation. Unfortunately, we found no crystal structures for 18-crown-6 complexes of silver in the literature. The only example was the silver nitrate complex of dibenzo-18-crown-6 (db18c6) [25]. Therefore, we performed calculations for $AgNO_3$:18c6 and used the crystal structure of $AgNO_3$:db18c6 for a qualitative comparison.

2. Method of calculation

Systems as large as crown ether complexes of heavy metals require much computational effort. The problem is additionally complicated by the fact that both electron correlation and relativistic effects should be treated properly. These difficulties make common ab initio methods inapplicable in this case. On the other hand, semi-empirical methods are unreliable for the systems of this type. A good alternative is

the use of DFT, which has been finding wider acceptance in studying heavy metal complexes [26–33].

Calculations were performed using the Amsterdam Density Functional (ADF) program package [34–38]. The density functional Hamiltonian contained the local density part (LDA) with the Vosko–Wilk–Nusair parametrization and the Becke (Becke88) nonlocal gradient corrections for the exchange part. The Perdew–Wang (DFT/BPW91) or Lee–Yang–Parr (DFT/BLYP) nonlocal corrections were used for the correlation part of the exchange-correlation potential. The relativistic effects were taken into account with the use of the quasi-relativistic scalar Pauli Hamiltonian implemented in ADF. Because of the use of the frozen core approximation in ADF, scalar relativistic effects are directly included in the Hamiltonian unless the valence basis is made extremely large. The core shells comprised up to and including the 1s shell for C, O, and N, the 2p shell for Cl, the 3p shell for Br, the 4p shell for I and Ag, and the 5p shell for Hg. The Slater-type basis set of triple-zeta quality with polarization functions included for light atoms (ADF, basis set IV) was used in the calculations. For complexes containing anionic ligands (NO_3^- or X^-), we did not include diffuse functions, because the total charge of these complexes was zero.

For free 18-crown-6 and for the anion-free complexes, we compared our DFT (BPW91 and BLYP) results with ab initio calculations within the second order Møller–Plesset perturbation theory (MP2). These calculations were performed using the GAMESS program package [39]. For C, O, and H atoms, we used 6-31G* basis set. For metal atoms, we used small-core quasi-relativistic Stuttgart ECPs (StR-sc ECP) and original (8s7p6d)/[6s5p3d] basis sets [40]. Since GAMESS cannot operate with functions with large angular momenta, the mercury ECP *g*-component was excluded from the original ECP.

Full geometry optimization was performed in the BPW91 and BLYP calculations of all considered systems and in the MP2 calculations of free 18-crown-6. The MP2/ECP calculations of anion-free complexes were performed for the geometries optimized at the BLYP level. The optimized geometrical structures were analysed and compared with experimental crystal structure data [41,42]. Unless otherwise specified, no symmetry restrictions were imposed during geometry optimization.

The adiabatic formation energies of complexes were calculated as the difference between the calculated energy of the optimized structure of the complex and the sum of the energies of the individual fragments. In this case, the energies of the corresponding polyatomic fragments were calculated at their optimized geometries. The vertical formation energies were calculated in the same way, but the energies of the individual fragments were in this case calculated at the geometries that these fragments assume in the complex.

The interaction energies of free 18-crown-6 and MX_y ($MX_y = AgNO_3$, $HgCl_2$, $HgBr_2$, and HgI_2) calculated by DFT/BPW91 were analysed within the Morokuma scheme of energy decomposition into contributions from Pauli, electrostatic, and orbital interactions according to Refs. [26–28,43]. The decomposition scheme operates with the vertical complex formation energies, which differ from the adiabatic complex formation energy by the energy of relaxation of the fragments to their equilibrium geometries.

The electron density distribution in the calculated complexes was analysed here in terms of Mulliken charges. Although the Mulliken charges sometimes do not describe the actual charge distribution, they may indicate some important general trends like charge transfer effects.

3. Results and discussion

3.1. Geometrical structure of the free 18-crown-6

According to the majority of X-ray crystal structure data, 18-crown-6 can exist in two main conformations, C_i and D_{3d} (Fig. 1). The prolate C_i conformation is observed for crystals of individual 18-crown-6 [44,45]. Experimental (IR, NMR, etc.) and molecular simulation data indicate that in nonpolar solvents 18-crown-6 adopts the same conformation [46–48]. On the contrary, in polar solvents 18-crown-6 prefers the D_{3d} conformation in which all oxygen atoms point into the crown ether cavity [46–53]. In crystals obtained by co-crystallization with polar solvents [54–63], 18-crown-6 also adopts the D_{3d} conformation. In crystals with highly polar molecules forming hydrogen bonds with crown ether oxygen atoms, the

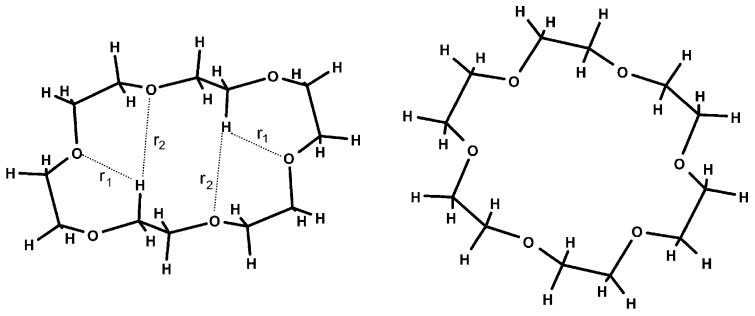

Fig. 1. Conformations of free 18-crown-6: (a) C_i and (b) D_{3d}. Dotted lines denote short H···O distances.

structure of 18-crown-6 can be severely distorted [64–66]. Therefore, the structural data on the D_{3d} conformation exhibit substantial scatter. We selected the least distorted experimental structures without inter or intramolecular hydrogen bonding [54–63]. For comparison with computational results, the structural data were averaged over the chosen set of structures.

The results of DFT (BPW91 and BLYP) and MP2/6-31G* calculations of the geometrical structure and relative energies of 18-crown-6 conformers are given in Table 1 together with the corresponding experimental geometrical parameters. An important property of crown ethers is the size of their cavity. The selectivity of crown ether interaction with various ions is determined by the correspondence of the ion size and the size of the crown ether cavity. The cavity size of 18-crown-6 is commonly characterised by the distances between the opposite oxygen atoms. The corresponding values are also given in Table 1. Because all the C, O, and H atoms in the D_{3d} conformation are equivalent by symmetry, whereas atoms in the C_i conformation are not all equivalent, we give average distances for the D_{3d} conformation and all nonequivalent distances for the C_i conformation.

In general, our calculated bond lengths for both conformations are in good agreement with the experimental data [44,45,54–63]. Though the bond lengths calculated at the DFT/BPW91 level are systematically larger than the corresponding experimental values, the relative error in bond lengths is rather small and lies almost within the experimental range.

The best agreement with the experimental bond lengths is achieved in DFT/BLYP calculations. The bond lengths calculated for the D_{3d} conformation at the MP2/6-31G* level are slightly overestimated in comparison to the experimental data, and the obtained accuracy in this case is intermediate between DFT/BPW91 and DFT/BLYP results. The MP2/6-31G* bond lengths for the C_i conformation are also in good agreement with the experiment.

A comparison with the experimental data shows that both DFT (BPW91 and BLYP) and MP2 methods overestimate the cavity size in the D_{3d} conformation (that is, the average cavity diameter) and the short O···O distance in the C_i conformation. This overestimation is rather large in DFT/BPW91 and DFT/BLYP calculations, especially for the short O···O distance in the C_i conformation. It is interesting to note that the long O···O distances in the C_i conformation are predicted to a good accuracy in both DFT/BPW91 and DFT/BLYP calculations. Thus, the C_i conformation predicted by DFT/BPW91 and DFT/BLYP is much less oblate than it is found in the experiment. Ab initio MP2/6-31G* calculations give here much better agreement with the experimental data. As a whole, MP2/6-31G* predicts shorter nonbonded interatomic distances for both 18-crown-6 conformations, so the calculated structures of the conformers are more compact than those predicted in both DFT/BPW91 and DFT/BLYP calculations.

As estimated by DFT/BPW91, the D_{3d} conformation is 1.6 kcal/mol lower in energy than the C_i conformation. On the contrary, DFT/BLYP and MP2/6-31G* predict that the D_{3d} conformation is, respectively, 1.1 and 7.2 kcal/mol higher in energy than the C_i structure. Whereas DFT (BPW91 and BLYP) methods predict that these two conformations

Table 1
Calculated (DFT and MP2/6-31G*) and experimental geometrical parameters of 18-crown-6-ether and relative conformational energies ΔE. Relative errors and uncertainties in bond lengths are given in parentheses

Conformation	D_{3d}[a]				C_i[b]			
Method	DFT BPW91	DFT BLYP	MP2/6-31G*	Experimental	DFT BPW91	DFT BLYP	MP2/6-31G*	Experimental
ΔE (kcal/mol)	−1.6	1.1	7.2		0.0	0.0	0.0	
C–C (Å)	1.516 (2.2%)	1.501 (1.1%)	1.508 (1.6%)	1.484 ± 0.02 (±1.4%)	1.516 (0.7%)	1.500 (−0.4%)	1.509 (0.2%)	1.506
					1.522 (0.7%)	1.507 (−0.3%)	1.513 (0.1%)	1.511
					1.525 (0.9%)	1.510 (−0.1%)	1.515 (0.2%)	1.512
C–O (Å)	1.424 (2.8%)	1.414 (2.1%)	1.416 (2.2%)	1.385 ± 0.03 (±2.2%)	1.426 (0.6%)	1.415 (−0.2%)	1.417 (−0.07%)	1.418
					1.429 (0.4%)	1.418 (−0.4%)	1.421 (−0.2%)	1.424
					1.437 (0.6%)	1.426 (−0.2%)	1.430 (0.07%)	1.429
Cavity size O–O (Å)	5.87 (3.5%)	5.83 (2.8%)	5.70 (0.5%)	5.67 ± 0.3 (±5.3%)	4.66 (10.4%)	4.64 (10.0%)	4.37 (3.6%)	4.22
					6.90 (0.9%)	6.78 (−0.9%)	6.76 (−1.2%)	6.84
					7.07 (1.4%)	7.02 (0.7%)	6.88 (−1.3%)	6.97

[a] Average distances.
[b] Nonequivalent distances.

Table 2
Geometrical parameters of Ag^+:18c6, Ag^0:18c6, Hg^{2+}:18c6, Hg^+:18c6, and Hg^0:18c6 complexes calculated by DFT

Complex	Ag^+:18c6		Ag^0:18c6		Hg^{2+}:18c6		Hg^+:18c6		Hg^0:18c6	
Method	BPW91	BLYP	BPW91	BLYP	BPW91	BLYP	BPW91	BLYP	BPW91	BLYP
C–C (Å)	1.507	1.491	1.521	1.505	1.503	1.487	1.512	1.498	1.527	1.512
C–O (Å)	1.435	1.425	1.430	1.419	1.446	1.435	1.438	1.427	1.433	1.421
M–O (Å)	2.79	2.77	2.99	2.97	2.81	2.77	2.90	2.87	3.08	3.05
Cavity size O···O (Å)	5.58	5.54	5.98	5.93	5.62	5.54	5.81	5.75	6.15	6.09

are rather close in energy, the MP2 calculations definitely predict that the C_i conformation is more stable. This is in agreement with the experimental data that 18-crown-6 prefers the C_i conformation in the absence of polar interactions. As was discussed in Refs. [14–16,21], the relative stability of the C_i structure is due to the intramolecular C–H···O attraction, which is not observed in the D_{3d} structure (see Fig. 1). According to the experimental data [44,45], there are rather short C–H···O contacts ($r_1 = 2.46$ and $r_2 = 2.64$ Å) in the C_i conformation of 18-crown-6. The calculated MP2 distances are 2.40 and 2.62 Å, respectively, that is, even shorter than in the experiment. DFT calculations give 2.47 and 2.92 Å (BLYP) and 2.50 and 2.90 Å (BPW91) for r_1 and r_2, respectively.

We note that the size of the crown ether cavity is mainly determined by the long-range (that is, nonbonded)] intramolecular interactions between links of the polyether cycle. It is known [67–71] that the commonly used density functionals, as a rule, inadequately describe long-range van der Waals-type interactions. At the same time, MP2 includes (and, possibly, overestimates) dynamic electron correlation effects, which account for the dispersion interaction. The underestimation of this interaction between distant atoms by DFT may be the reason for the overestimation of the calculated cavity size in the D_{3d} conformation and the short O···O distance in the C_i conformation, and, hence, for the small (and even negative for DFT/BPW91) relative conformational energy calculated for the D_{3d} structure.

3.2. Anion-free complexes and reduction of Ag^+, Hg^+, and Hg^{2+} captured in the crown ether cavity

The calculated structures of anion-free crown ether complexes of silver and mercury are given in Table 2. Experimental data indicate that metal complexes of 18-crown-6 in polar media mostly assume the D_{3d} conformation [41,42]. Therefore, we considered only the D_{3d} conformation of the silver and mercury 18-crown-6 complexes and used the D_{3d} structure of free 18-crown-6 as a reference point. The geometry of neutral complexes was optimized under the restriction that the structure remains centrally symmetric.

As compared to the free crown ether, the C–C bonds in the cationic metal complexes are shortened, and the C–O bonds are lengthened. The same theoretical results were obtained for alkali and alkaline-earth metal complexes of 18-crown-6 [14–16]. In addition, the similar general trends were obtained for some protonated polyethers, including 18-crown-6 [21]. The cavity in the closed-shell cationic complexes is contracted compared to free 18-crown-6 by ~0.25 Å for both Ag^+:18c6 and Hg^{2+}:18c6 and by ~0.07 Å for Hg^+:18c6. It is interesting to note that the geometrical characteristics of the closed-shell cationic Ag^+:18c6 complex, including both the bond lengths and the cavity size, are close to those of the (closed-shell) Hg^{2+}:18c6 complex rather than to the similarly charged open-shell Hg^+:18c6.

The successive reduction of the closed-shell cationic complexes to the neutral ones results in an increase in the bond lengths and in a significant increase in the cavity size, which finally becomes considerably larger than in free 18-crown-6. The geometrical characteristics of the neutral Ag^0:18c6 are intermediate between those of Hg^+:18c6 and Hg^0:18c6. Thus, the crown ether cavity is expanded by ~0.1 Å in Ag^0:18c6 and by ~0.27 Å in Hg^0:18c6 as compared to the free 18-crown-6, whereas in Hg^+:18c6 it is contracted by ~0.06 Å.

The calculated formation energies are given in Table 3. Generally, the interaction between the central

Table 3
Bonding energies E_b for anion-free complexes (eV)

Complex	BPW91	BLYP	MP2[a]
Ag^+:18c6	3.72	4.11	4.93
Ag^0:18c6	−0.43	−0.21	0.49
Hg^{2+}:18c6	12.13	12.59	11.87
Hg^+:18c6	3.46	3.86	4.36
Hg^0:18c6	−0.87	−0.66	0.07

[a] MP2/6-31G*/St-RSc ECP, geometry optimized by BLYP.

metal ion (atom) and the crown ether ligand is determined by the following physically different attractive and repulsive contributions: (1) attractive electrostatic, charge transfer, and orbital interactions, (2) Pauli repulsion, and (3) attractive van der Waals interactions. Commonly, van der Waals interactions are not separated in the conventional energy decomposition schemes [43]. However, it is well known that intramolecular closed-shell interactions of van der Waals-type are very important and could be structure-determining in heavy metal compounds [13]. It is quite natural to expect that the relative contribution of electrostatic and charge transfer interactions will increase with increasing formal charge of the central ion and, on the contrary, the relative contribution of van der Waals-type interactions will increase for complexes with neutral metal atoms.

It can be seen from Table 3 that the calculated formation energies are rather close to each other for equally charged ions. However, the metal–ligand bonding energies (E_b(M–L) = $-E_f$) for Ag^+ and Ag^0 are systematically higher than the corresponding values for Hg^+ and Hg^0 in all variants of calculations. This behaviour can be explained by the fact that mercury has one additional s-electron on its outer s-orbital compared to silver, which should increase the effects of Pauli repulsion between the central atom (ion) and the ligand.

On the other hand, the formation energies strongly depend on the formal charge of the central ion and decrease drastically as it decreases from +2 to +1 and, then, to 0. This dependence is strongly nonlinear. All methods consistently predict that the increase in the charge of the central atom from 0 to +1 results in an increase in the complex formation energies by ~4.2–4.4 eV for silver and 4.3–4.5 eV for mercury. The increase of the calculated formation energy of the Hg^{2+} complex compared to the Hg^+ complex is much larger (~8.7 eV in DFT/BPW91 and DFT/BLYP calculations and ~7.5 eV in MP2).

The DFT/BPW91 and DFT/BLYP calculations

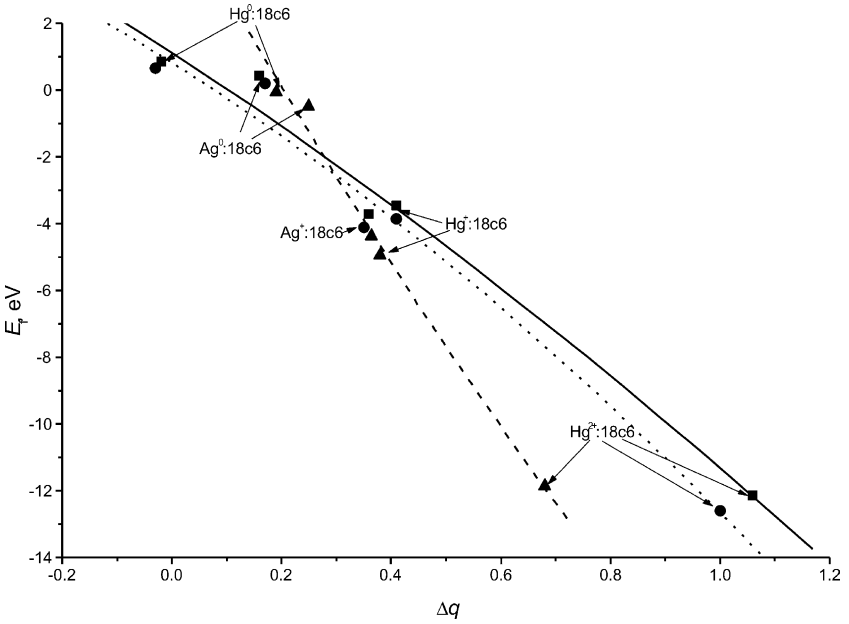

Fig. 2. Calculated complex formation energies E_f vs. electron transfer Δq from the ligand to the central atom. ■ BPW, ● BLYP, ▲ MP2.

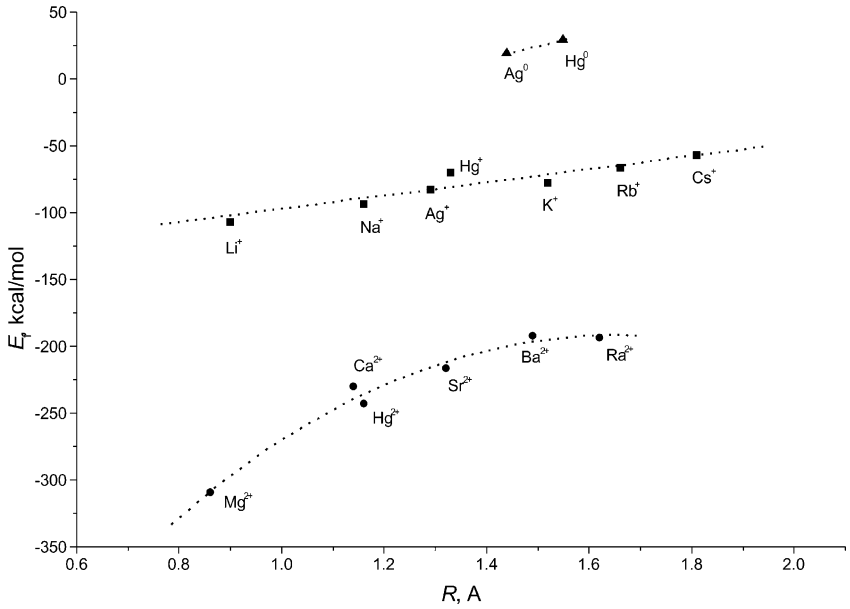

Fig. 3. Complex formation energy E_f (MP2/6-31 + G*) for M^{n+}:18c6 as a function of ionic radius R for (■) singly charged ions, (●) doubly charged ions, and (▲) atoms.

predict that the bonding energies of neutral complexes are negative; that is, the corresponding complexes are unstable with respect to dissociation. At the same time, the MP2 calculated bonding energies of neutral complexes are positive (0.49 eV for Ag^0:18c6 and 0.07 eV for Hg^0:18c6). Generally, the metal–ligand bonding energies calculated by different methods increase in the following sequence: $E_b(MP2) > E_b(BLYP) > E_b(BPW91)$. The only exception is the MP2 value for the Hg^{2+}:18c6 complex. We associate this general behaviour with intramolecular van der Waals-type interaction, which is not properly reproduced by the commonly used DFT functionals. At the same time, these interactions make an important contribution to the metal–ligand bonding energy for metals in low oxidation states. Therefore, we may expect that, according to MP2 calculations, the neutral complexes are actually characterised by some positive bonding energy E_b(M–L), at least, in the case of silver. This result is in agreement with the experimental findings [10–12], where it was found that the neutral silver atom can be retained in the cavity of a crown ether.

The formation of 18-crown-6 complexes from the metal cation (or atom) and the crown ether (M^{n+} + 18c6) results in considerable electron density transfer from the ligand to the metal. This electron transfer makes a significant contribution to the metal–ligand interaction in the case of highly charged complexes (see Fig. 2). A good, almost linear correlation is observed between the ligand → metal electron density transfer and the complex formation energies. One can see that the slope of the line corresponding to the MP2 calculation is greater than that of the lines corresponding to DFT/BPW91 and DFT/BLYP, and the range of electron transfer values for MP2 is much smaller. It is seen in Fig. 2 that MP2/6-31G* calculation predicts much smaller charge transfer effects in the complexes, which are mainly responsible for the bonding energy in the case of the doubly charged Hg^{2+}:18c6 complex. This may explain why the formation energy of Hg^{2+}:18c6 calculated by MP2 is anomalously smaller than that calculated by the DFT/BPW91 and DFT/BLYP methods.

It is commonly believed that the complex formation energies for a given crown ether correlate with the ionic radius of the central ion. Though our results for the heavy d-block metals cannot be compared directly with experimental data, we may consider now overall correlation between the calculated complex formation energies and the ionic radii. We

Table 4
Experimental and calculated electron affinities of Ag and Hg cations (with relative errors given in parentheses) and calculated adiabatic electron affinities of Ag and Hg complexes with 18-crown-6 (in eV)

Ion	Experimental	BPW91	BLYP	MP2
Ag^+	−7.58	−8.02 (5.8%)	−9.01 (18.9%)	−6.82 (−10.0%)
Hg^+	−10.44	−10.39 (−0.5%)	−11.69 (12.0%)	−9.04 (−13.4%)
Hg^{2+}	−18.76	−19.10 (1.8%)	−20.26 (8.0%)	−16.94 (−9.7%)
Ag^+:18c6		−3.87	−4.69	−2.38[a]
Hg^+:18c6		−6.05	−7.17	−4.75[a]
Hg^{2+}:18c6		−10.43	−11.53	−9.43[a]

[a] MP2/6-31G*/St-RSc ECP, geometry optimized by BLYP.

include in this correlation the formation energies for crown ether complexes of alkali and alkaline-earth metals calculated in Refs. [14–16], which are in a good agreement with the available gas-phase experimental data [17–20]. Fig. 3 presents the MP2/6-31G* formation energies for anion-free 18-crown-6 complexes of silver and mercury calculated in this work along with the MP2/6-31 + G* results for similar complexes of alkali and alkaline-earth metals against the ionic radii (or metallic radii for neutral atoms) taken from Refs. [72,73]. The formation energies fall into groups corresponding to similarly charged ions (neutral atoms), whereas the formation energies within each particular group correlate well with the ionic (metallic) radii. The data for d-block metal (silver and mercury) ions are described well by the same lines as the (similarly charged) alkali or alkaline-earth metal ions. This fact supports the idea that, at least in the case of 18-crown-6, the ion size rather than chemical specificity of an ion determines its affinity to the crown ether.

The calculated adiabatic electron affinities for 18-crown-6 complexes of Ag^+, Hg^+, and Hg^{2+} given in Table 4 indicate that the metal ions (at least, in the gas-phase) can capture an electron inside the crown ether cavity. However, there are large discrepancies in electron affinities calculated by different methods. In order to explain these discrepancies, consider the electron affinities of the corresponding free ions given in the same table. Compared to the experimental values [74], the electron affinities of free cations obtained at the DFT/BLYP level are strongly overestimated, and the values obtained at the MP2/6-31G* level are strongly underestimated. The DFT/BPW91 values are in much better agreement with the experiment, though the calculated electron affinities for Ag^+ and Hg^{2+} are still somewhat larger than the experimental ones.

It is well known that ab initio methods commonly underestimate ionization potentials. This underestimation is generally explained by the underestimation of the correlation energy in ab initio calculations, which is larger in the systems with a greater number of electrons. On the contrary, the overestimation of electron affinities obtained in DFT methods indicate that these methods underestimate the relative stability of the Ag^+ and Hg^{2+} $(n-1)d^{10}ns^0$ states with respect to their parentage Ag^0 and Hg^+ $(n-1)d^{10}ns^1$ states.

This, at first glance anomalous behaviour of DFT calculations deserves some general comments. In both Ag^+ and Hg^{2+} ions, the outer s-orbital is vacant and lies relatively low with respect to the outer occupied d-orbitals (…$4d^{10}s^0$ and …$5d^{10}s^0$ configurations, respectively). Therefore, the main contribution to the correlation energy of the ground states of these ions is made by $d^2 \rightarrow s^2$ excitations. These excitations should transfer electron density onto the lowest outer *n*s-orbital of the corresponding ions. However, this transfer cannot be easily reproduced within the Kohn–Sham one-electron approach for the spherically symmetric $(n-1)d^{10}ns^0$ states, because, in this case, symmetry restrictions prevent the *n*s orbital from mixing with $(n-1)$d orbitals. It might be believed that the *n*s-contribution to the total one-electron density could be approximately described by allowing the $(n-1)$d-shell to expand through adding diffuse d functions. We checked this possibility and found that including additional diffuse d components into the basis set does not improve the results for atomic ionisation potentials. This failure is most probably due to

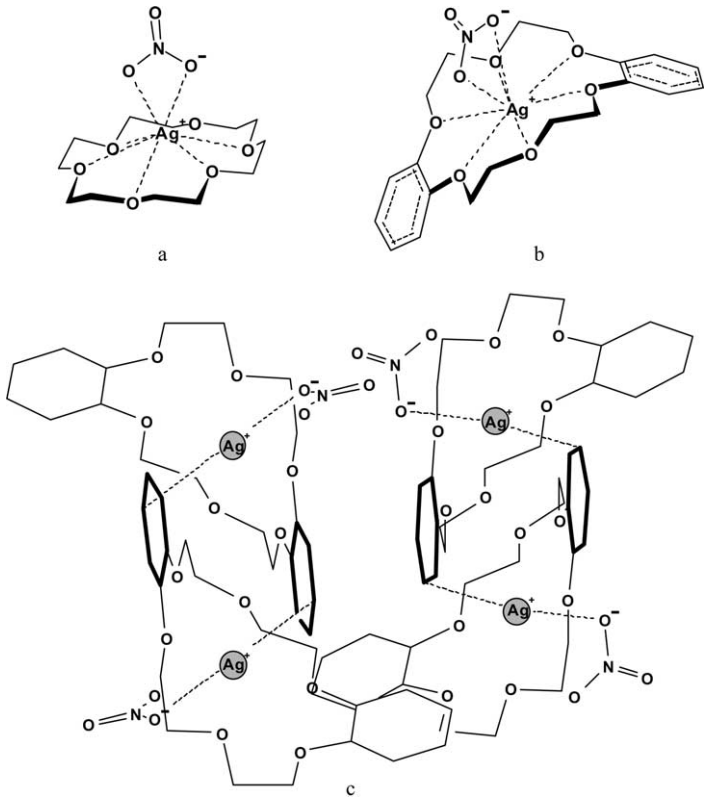

Fig. 4. Calculated structure of (a) $AgNO_3$:18c6, experimental structure of (b) $AgNO_3$:db18c6, and a fragment of the crystal structure (c) of $AgNO_3$:db18c6 showing $C^{ar}\cdots$Ag–O close contacts (dashed lines) and stacking of the benzene rings (bold lines).

the fact that the kinetic energy term corresponding to d-orbitals is considerably larger than that corresponding to s-orbitals with the same spatial localisation. It is well known that the exchange-correlation potentials within the Kohn–Sham theory must include a kinetic energy part [75]. This part, however, cannot be tuned easily to describe this situation, though from a theoretical point of view a corresponding functional could be constructed in principle [76]. Therefore, it is reasonably expected that DFT with the currently available exchange-correlation potentials should underestimate the correlation energies of closed-shell ions of this type.

On the other hand, the picture in the case of the $(n-1)d^{10}ns^1$ states with one additional electron (Ag^0 and Hg^+) is completely different. Now, $(n-1)d \rightarrow ns$ transitions give no lowest-order contributions to the correlation energy. One-electron $d^1 \rightarrow s^1$ terms are zero by symmetry restrictions, and two-electron $d^2 \rightarrow s^2$ terms are simply absent, because the ns-orbital is now semi-occupied. Therefore, there is no $d \rightarrow s$ electron density transfer in this case. Hence, in the case of the $(n-1)d^{10}ns^1$ states, there is no sources of the systematic error discussed above in DFT calculations. Thus, we may expect that the electron affinity calculated within the Kohn–Sham theory should always be overestimated for the closed-shell system in which the HOMO and LUMO of different symmetry are close in energy to each other. This explains the overestimation of the electron affinities of the $(n-1)d^{10}ns^0$ states, which is observed in both DFT/BPW91 and DFT/BLYP methods. Having this in mind, we may conclude that the BPW91 functional gives quite reasonable agreement between the calculated and the experimental electron affinities and may also consider the electron affinities obtained with this functional for crown ether complexes reliable.

Table 5
Geometrical parameters of $AgNO_3$:18c6 calculated by DFT

Complex	$AgNO_3$:18c6		$AgNO_3$:db18c6
Method	BPW91	BLYP	(Experimental)
C–C (Å)	1.512	1.496	1.516 ± 0.018[a]
C–O (Å)	1.430	1.419	1.446 ± 0.017[b]
Ag–O (crown) (Å)	2.92[c]	2.89[c]	2.74[d]
	3.11[c]	3.07[c]	2.75[d]
Cavity size O···O (Å)	5.72	5.67	5.48
Out-of-plane h[e] (Å)	0.95	0.92	0.0
Ag–O (NO_3^-) (Å)	2.37	2.36	2.49[d]
			2.44[d]

[a] Single C–C bonds.
[b] O atoms not conjugated with benzene rings.
[c] Nonequivalent distances.
[d] In different subunits.
[e] Average height of O–Ag–O triangles.

From the above discussion and the results shown in Table 4, we may state that DFT mainly overestimates electron affinities, whereas MP2 underestimates them. It is this underestimation that is the reason for smaller charge transfer effects and, hence, for the smaller bonding energy predicted by MP2 for the Hg^{2+}:18c6 complex as compared with DFT/BPW91 and DFT/BLYP calculations (see Fig. 2 and discussion above).

3.3. Neutral crown ether complexes of silver(I) and mercury(II) with anionic ligands

Crown ether complexes in a condensed phase are surrounded by counterions or solvent molecules. The interaction of the central ion with these additional charged or polar ligands may affect both the metal–crown bonding energy and the redox properties of the complexed heavy metal ions.

The calculated structure of $AgNO_3$:18c6 and experimental structure of $AgNO_3$:db18c6 are shown in Fig. 4, and the corresponding geometrical parameters are given in Table 5. The calculated C–C and C–O bond lengths are within the scatter of the experimental data, whereas the calculated cavity size is ~0.20 to 0.25 Å larger than the experimental value (similar to the results obtained for the free crown ether). The bond lengths and cavity size in the crown ether moiety of $AgNO_3$:18c6 are intermediate between those for the anion-free cationic complex and the free crown ether.

The calculation predicts that the NO_3^- anion is coordinated to Ag^+ through two oxygen atoms (bifurcated coordination). In the calculated structure, the NO_3^- anion pulls the Ag^+ cation out of the (average) plane of crown ether oxygen atoms (see Table 5 and Fig. 4). The out-of-plane displacement can be characterised by the average height of the O–Ag–O triangles based on two opposite crown ether oxygen atoms. In the experimental structure, Fig. 4b, the anion coordination to Ag^+ is unsymmetrical. One of the Ag–O distances is shorter than the other ones, and the Ag^+ cation resides in the (average) plane of oxygen atoms. The calculated Ag–O distances are ~0.1 Å shorter than the shortest Ag–O distance in the experimental structure. Thus, it is qualitatively evident that the electrostatic interaction between the NO_3^- anion and the central ion in the calculated geometry should be much stronger than that in the experimental geometry.

It should be noted that the experimental crystal structure of $AgNO_3$:db18c6 [25] is characterised by very short $Ag^+\cdots C^{ar}$ contacts between Ag^+ and the aromatic ring of the neighbouring molecular subunits (2.63 and 2.80 Å for two nonequivalent molecules in the crystal cell, Fig. 4c). The C^{ar}, Ag^+, and ONO_2^- form an approximately linear $C^{ar}\cdots Ag–O$ fragment, so that the coordination of Ag^+ corresponds to a bipyramidal structure with crown ether in equatorial position and C^{ar} and O occupying opposite axial positions. The $Ag^+–ONO_2^-$ distance in the experimental structure inversely correlates with the $Ag^+\cdots C^{ar}$ distance (Ag–O 2.49 and Ag···C 2.63 Å in one subunit, and Ag–O 2.44 and Ag···C 2.80 Å in the other subunit). It can be argued that the intermolecular $Ag\cdots C^{ar}$ interaction may be responsible for the weakening of the $Ag^+–ONO_2^-$ bond in the experimental structure. Thus, the existence of the additional $C^{ar}\cdots Ag^+$ interaction and the weakening of the $Ag^+–ONO_2^-$ interaction in the experimental structure may explain why Ag^+ remains within the plane of O atoms inside the crown ether cavity.

On the other hand, Cambridge Structural Database provides many examples of out-of-plane displacements of central ions in crown ether complexes similar to that observed in the calculated structure of $AgNO_3$:18c6 [77–81]. In all these examples, there is always an additional ligand coordinated to the central ion on one side of the crown ether fragment. Even

Table 6
Calculated (DFT) and experimental geometrical parameters of $HgCl_2$:18c6, $HgBr_2$:18c6, and HgI_2:18c6 complexes with mean relative errors in bond lengths given in parentheses

Complex	$HgCl_2$:18c6			$HgBr_2$:18c6			HgI_2:18c6		
Method	BPW91	BLYP	Experimental	BPW91	BLYP	Experimental	BPW91	BLYP	Experimental
C–C (Å)	1.518 (1.8%)	1.503 (0.8%)	1.491	1.518 (0.5%)	1.503 (−0.5%)	1.511	1.517 (2.1%)	1.503 (1.1%)	1.486
C–O (Å)	1.432 (1.2%)	1.421 (0.4%)	1.415	1.433 (1.8%)	1.421 (0.9%)	1.408	1.432 (1.2%)	1.421 (0.4%)	1.415
Hg–O (Å)	2.934 (3.9%)	2.904 (2.8%)	2.825	2.932 (3.4%)	2.904 (2.4%)	2.835	2.927 (2.1%)	2.900 (1.1%)	2.868
Cavity size O···O (Å)	5.87 (3.9%)	5.81 (2.8%)	5.65	5.86 (3.4%)	5.81 (2.5%)	5.67	5.86 (2.3%)	5.80 (1.2%)	5.73
Hg–X (Å)	2.437 (5.4%)	2.436 (5.3%)	2.313	2.590 (6.1%)	2.586 (6.0%)	2.440	2.868 (9.5%)	2.858 (9.1%)	2.619

Table 7
Complex formation energies (eV) for 18-crown-6 complexes with $AgNO_3$, $HgCl_2$, $HgBr_2$, and HgI_2 (calculated by BPW91) and Morokuma energy decomposition

Complex	Formation energy		Deformation energy	Pauli repulsion	Electrostatic attraction	Orbital interaction
	Adiabatic	Vertical				
$AgNO_3$:18c6	−1.012	−1.141	0.129	1.233	−1.648	−0.726
$HgCl_2$:18c6	−0.336	−0.422	0.086	2.332	−1.929	−0.825
$HgBr_2$:18c6	−0.233	−0.358	0.125	2.535	−1.997	−0.896
HgI_2:18c6	−0.248	−0.382	0.134	2.727	−2.078	−1.031

when the cation size fits perfectly the crown ether cavity size (like in the case of potassium), strong interaction between the cation and the additional ligand can draw the cation out of the crown ether plane. Thus, the potassium complexes with 18-crown-6 and molybdocene, ethylacetoacetate, or thiocyanato silver as another ligand are characterised by an out-of-plane displacement of ~0.7 to 0.9 Å [77–81].

The calculated and experimental [22–24] geometrical parameters of HgX_2:18c6 complexes are given in Table 6. The calculated parameters only slightly depend on the counterions. However, experimental data show that the cavity size in HgI_2:18c6 is somewhat larger than that in $HgCl_2$:18c6 and $HgBr_2$:18c6. Both the calculated and experimental bond lengths in the crown ether moiety of HgX_2:18c6 are consistently larger than the corresponding values for free 18-crown-6. The C–O bond lengths are more sensitive to the presence of the HgX_2 molecule in the cavity (they are stretched by ~0.03 Å). However, the cavity size in the complexes remains virtually the same as in free 18-crown-6 with the only exception of HgI_2:18c6, where the experimental cavity diameter is ~0.06 Å larger than that in 18-crown-6.

Unlike $AgNO_3$:18c6, the calculated Hg–X bond lengths in HgX_2:18c6 complexes are markedly larger than the experimental ones, and this overestimation increases from Cl to I. This can be attributed to the crystal effects. Crystalline HgX_2:18c6 complexes exhibit nonbonded X···X contacts between neighbouring HgX_2:18c6 molecular fragments. The X···X distance in these contacts decreases from Cl to Br and I. In the case of Cl^-, this distance is 6.63 Å, which is 3.29 Å larger than the sum of ionic radii of two neighbouring Cl^- ions. That is, the Cl···Cl nonbonded distances are rather long. In the case of Br^- and I^-, these distances (4.30 Å in both cases) are relatively short and only slightly exceed the sum of the corresponding ionic radii (by 0.66 Å for Br^- and 0.18 Å for I^-). Such short contacts are typical for heavy halide anions, which can participate in strong closed-shell interactions [13]. The short X···X contacts in the crystal enhance the donor ability of the X^- anion toward the Hg^{2+} cation in the Hg–X···X fragments and thus strengthen the Hg–X bond. Clearly, this effect cannot be reproduced in a gas-phase calculation.

Table 7 gives the energies of formation (E_f) of $AgNO_3$:18c6 and HgX_2:18c6 complexes from free crown ether and the MX_y fragment and the corresponding components defined within the Morokuma energy decomposition scheme [26–28,43]. Contrary to the naive idea that a doubly charged cation must interact more strongly with a ligand than a singly charged one, the formation energy for the $AgNO_3$:18c6 complex is much larger than for all the HgX_2:18c6 complexes. Though attractive electrostatic and orbital interactions are stronger in the case of HgX_2, the dominant effect is produced by the Pauli repulsion between MX_y molecule and the crown ether moiety. The Pauli repulsion in HgX_2 complexes is much larger than in the $AgNO_3$ complex and monotonically increases in the series $AgNO_3 < HgCl_2 < HgBr_2 < HgI_2$. This increase in Pauli repulsion determines the lower formation energy for mercury halide complexes.

This behaviour can be related with the fact that the central ion in the unsymmetrical $AgNO_3$:18c6 complex can be displaced from the macrocycle plane, which reduces the Pauli repulsion between $AgNO_3$ and crown ether. On the contrary, the central symmetry of HgX_2:18c6 complexes precludes this kind of displacement. Two anionic ligands arranged

on both sides of the Hg^{2+} cation keep it firmly in the macrocycle plane and, therefore, the Pauli repulsion between the Hg^{2+} cation and crown ether cannot be reduced in this case.

4. Conclusions

The electronic and geometrical structure of 18-crown-6 and its complexes with silver and mercury is studied by DFT (BPW91 and BLYP) and MP2 calculations. We have analysed factors determining the relative stability of conformations of 18-crown-6 and the stability of crown ether complexes with and without counterions. The MP2 and BLYP methods describe the geometry of free crown ether rather well, and the relative stability of the conformations studied is in a good agreement with experiment. However, the DFT methods do not properly describe long-range interactions, which are important for the free crown ether and its complexes with neutral atoms and molecules. As expected, the Hg^{2+} ion is most strongly bound to the crown ether; the bonding energies of the singly charged Hg^{+} and Ag^{+} ions are rather close to each other. Silver and mercury ions in the 18-crown-6 cavity can capture an electron, and Ag^{0}:18c6 can be bound through van der Waals-type interactions, whereas the bonding in Hg^{0}:18c6 is rather weak. The stability of metal complexes with anionic ligands is not determined by the cation charge but mainly by the mode of coordination of the anionic ligands to the central metal ion. The HgX_2:18c6 complexes are less stable than $AgNO_3$:18c6, because the symmetric arrangement of the anionic ligands prevents the cation from being displaced out of the macrocycle plane. The stability of HgX_2:18c6 complexes only slightly depends on the anion X.

Acknowledgements

Financial support from the Royal Society, the Russian Foundation for Basic Research (projects No. 99-03-33180 and No. 02-03-32420) and the European Science Foundation (Relativistic Effects in Heavy Elements Programme) is gratefully acknowledged. The Licence for Cambridge Crystallographic Database is financially supported by Russian Foundation for Basic Research (project No. 99-07-90133). The authors thank Dr A.V. Churakov for his help in collecting crystallographic data. Professor J.A.K. Howard thanks the EPSRC for a senior research fellowship.

References

[1] V. Balzani, A. Credi, M. Venturi, Coord. Chem. Rev. 171 (1998) 3.
[2] S.P. Gromov, M.V. Alfimov, Russ. Chem. Bull. 46 (1997) 611.
[3] M. Takeshita, C.F. Soong, M. Irie, Tetrahedron Lett. 39 (1998) 7717.
[4] S.H. Kawai, Tetrahedron Lett. 39 (1998) 4445.
[5] I.K. Lednev, R.E. Hester, J.N. Moore, J. Phys. Chem. A 101 (1997) 7371.
[6] I.K. Lednev, T.-Q. Ye, R.E. Hester, J.N. Moore, J. Phys. Chem. A 101 (1997) 4966.
[7] I.K. Lednev, R.E. Hester, J.N. Moore, J. Am. Chem. Soc. 119 (1997) 3456.
[8] R. Bergonzi, L. Fabrizzi, M. Licchelli, C. Mangano, Coord. Chem. Rev. 170 (1998) 31.
[9] L.F. Lindoy, Coord. Chem. Rev. 174 (1998) 327.
[10] R. Humphry-Baker, M. Gratzel, P. Tundo, E. Pelizzetti, Angew. Chem. Int. Ed. Engl. 18 (1979) 630.
[11] M. Gubelmann, A. Harriman, J.-M. Lehn, J.L. Sessler, J. Chem. Soc., Chem. Commun. (1988) 77.
[12] M. Gubelmann, A. Harriman, J.-M. Lehn, J.L. Sessler, J. Phys. Chem. 94 (1990) 308.
[13] P. Pyykkö, Chem. Rev. 97 (1997) 597.
[14] E.D. Glendening, D. Feller, M.A. Thompson, J. Am. Chem. Soc. 116 (1994) 10657.
[15] E.D. Glendening, D. Feller, J. Am. Chem. Soc. 118 (1996) 6052.
[16] D. Feller, A. Eldorado, J.A. Nichols, D.E. Bernholdt, J. Chem. Phys. 105 (1996) 1940.
[17] B.M. More, E.D. Glendening, D. Ray, D. Feller, P.B. Armentrout, J. Phys. Chem. 100 (1996) 1605.
[18] D. Ray, D. Feller, B.M. More, E.D. Glendening, P.B. Armentrout, J. Phys. Chem. 100 (1996) 16116.
[19] S.E. Hill, E.D. Glendening, D. Feller, J. Phys. Chem. A 101 (1997) 6125.
[20] S.E. Hill, D. Feller, E.D. Glendening, J. Phys. Chem. A 102 (1998) 3813.
[21] H. Wasada, Y. Tsutsui, S. Yamabe, J. Phys. Chem. 100 (1996) 7367.
[22] C.R. Paige, M.F. Richardson, Can. J. Chem. 62 (1984) 332.
[23] R.D. Rogers, A.H. Bond, J.L. Wolff, J. Coord. Chem. 29 (1993) 187.
[24] M. El Essawi, S. Abd El Khalik, K.-F. Tebbe, Acta Crystallogr. Sect. C (Cr. Str. Comm.) 52 (1996) 818.
[25] Z. Liu, M. Shao, Beijing Dax. Xue., Zir. Kex. 6 (1987) 17.
[26] A. Rosa, E.J. Baerends, Inorg. Chem. 33 (1994) 584.
[27] T. Ziegler, A. Rauk, Theor. Chim. Acta 49 (1977) 143.
[28] T. Ziegler, A. Rauk, Inorg. Chem. 18 (1979) 1755.

[29] T. Ziegler, Chem. Rev. 71 (1991) 651.
[30] F. Ogliaro, J.F. Halet, D. Astruc, J.Y. Saillard, New J. Chem. 24 (2000) 257.
[31] K. Pierloot, A. Ceulemans, M. Merchan, L. Serrano-Andres, J. Phys. Chem. A 104 (2000) 4374.
[32] F.P. Liang, H. Jacobsen, H.W. Schmalle, T. Fox, H. Berke, Organometallics 19 (2000) 1950.
[33] N. Fey, J. Chem. Technol. Biotechnol. 74 (1999) 852.
[34] E.J. Baerends, D.E. Ellis, P. Ros, Chem. Phys. 2 (1973) 42.
[35] E.J. Baerends, P. Ros, Chem. Phys. 2 (1973) 51.
[36] E.J. Baerends, P. Ros, Int. J. Quantum Chem. S12 (1978) 169.
[37] P.M. Boerrigter, G. te Velde, E.J. Baerends, Int. J. Quantum Chem. 33 (1988) 87.
[38] G. te Velde, E.J. Baerends, J. Comput. Phys. 99 (1992) 84.
[39] M.W. Schmidt, K.K. Baldridge, J.A. Boatz, S.T. Elbert, M.S. Gordon, J.H. Jensen, S. Koseki, N. Matsunaga, K.A. Nguyen, S.J. Su, T.L. Windus, M. Dupuis, J.A. Montgomery, J. Comput. Chem. 14 (1993) 1347.
[40] D. Andrae, U. Haeussermann, M. Dolg, H. Stoll, H. Preuss, Theor. Chim. Acta 77 (1990) 123.
[41] Cambridge Structural Database, October 1999 version, Cambridge Crystallographic Data Centre, Cambridge, UK.
[42] F.H. Allen, J.E. Davies, J.J. Galloy, O. Johnson, O. Kennard, C.F. Macrae, E.M. Mitchell, G.F. Mitchell, J.M. Smith, D.G. Watson, J. Chem. Inf. Comput. Sci. 31 (1991) 187.
[43] K. Morokuma, J. Chem. Phys. 55 (1971) 1236.
[44] J.D. Dunitz, M. Dobler, P. Seiler, R.P. Phizackerly, Acta Crystallogr. B 30 (1974) 2733.
[45] E. Maverick, P. Seiler, W.B. Schweizer, J.D. Dunitz, Acta Crystallogr. B 36 (1980) 615.
[46] Y.L. Ha, A.K. Chakraborty, J. Phys. Chem. 95 (1991) 10781.
[47] Y.L. Ha, A.K. Chakraborty, J. Phys. Chem. 96 (1992) 6410.
[48] Y.L. Ha, A.K. Chakraborty, J. Phys. Chem. 97 (1993) 11291.
[49] D. Live, S.I. Chan, J. Am. Chem. Soc. 98 (1976) 3769.
[50] P.A. Mosier-Boss, A.I. Popov, J. Am. Chem. Soc. 107 (1985) 6168.
[51] S.A. Bryan, R.R. Willis, B.A. Moyer, J. Phys. Chem. 94 (1990) 5230.
[52] R. Begum, T. Yonemitsu, H. Matsuura, J. Mol. Struct. 447 (1998) 111.
[53] K. Patil, R. Pawar, J. Phys. Chem. B 103 (1999) 2256.
[54] J.A.A. de Boer, D.N. Reinhoudt, S. Harkema, G.J. van Hummel, F. de Jong, J. Am. Chem. Soc. 104 (1982) 4073.
[55] R.D. Rogers, L.M. Green, J. Inclusion Phenom. 4 (1986) 77.
[56] R.D. Rogers, P.D. Richards, J. Inclusion Phenom. 5 (1987) 631.
[57] R.D. Rogers, P.D. Richards, E.J. Voss, J. Inclusion Phenom. 6 (1988) 65.
[58] R.L. Garrell, J.C. Smyth, F.R. Fronczek, R.D. Gandour, J. Inclusion Phenom. 6 (1988) 73.
[59] F. Weller, H. Borgholte, H. Stenger, S. Vogler, K. Dehnicke, Z. Naturforsch. Teil B 44 (1989) 1524.
[60] G. Weber, J. Mol. Struct. 98 (1983) 333.
[61] I. Goldberg, Acta Crystallogr. Sect. B 31 (1975) 754.
[62] J.A. Bandy, M.R. Truter, F. Vogtle, Acta Crystallogr. Sect. B 37 (1981) 1568.
[63] A. Elbasyouny, H.J. Brugge, K. von Deuten, M. Dickel, A. Knochel, K.U. Koch, J. Kopf, D. Melzer, G. Rudolph, J. Am. Chem. Soc. 105 (1983) 6568.
[64] J.W.H.M. Uiterwijk, G.J. van Hummel, S. Harkema, V.M.L.J. Aarts, K. Daasvatn, J. Geevers, H.J. den Hertog Jr., D.N. Reinhoudt, J. Inclusion Phenom. 6 (1988) 79.
[65] J.W.H.M. Uiterwijk, S. Harkema, D.N. Reinhoudt, K. Daasvatn, H.J. den Hertog Jr., J. Geevers, Angew. Chem. Int. Ed. Engl. 21 (1982) 450.
[66] S. Harkema, G.J. van Hummel, K. Daasvatn, D.N. Reinhoudt, J. Chem. Soc. Chem. Commun. (1981) 368.
[67] B.I. Lundqvist, Y. Andersson, H. Shao, S. Chan, D.C. Langreth, Int. J. Quantum Chem. 56 (1995) 247.
[68] Y. Andersson, D.C. Langreth, B.I. Lundqvist, Phys. Rev. Lett. 76 (1996) 102.
[69] E. Hult, Y. Andersson, D.C. Langreth, B.I. Lundqvist, Phys. Rev. Lett. 77 (1996) 2029.
[70] Y. Andersson, E. Hult, P. Apell, D.C. Langreth, B.I. Lundqvist, Solid State Commun. 106 (1998) 235.
[71] B.I. Lundqvist, E. Huld, H. Rydberg, A. Bogicevic, J. Strömquist, D.C. Langreth, Progr. Surf. Sci. 59 (1998) 149.
[72] R.D. Shannon, C.T. Prewitt, Acta Crystallogr. B 25 (1969) 925.
[73] R.D. Shannon, Acta Crystallogr. A 32 (1976) 751.
[74] C.E. Moore, Ionization Potentials and Ionization Limits Derived from Optical Spectra, National Standard Reference Data Series, vol. 34, National Bureau of Standards, Washington, 1970.
[75] E.J. Baerends, O.V. Gritsenko, J. Phys. Chem. A 101 (1997) 5383.
[76] P.R.T. Schipper, O.V. Gritsenko, E.J. Baerends, Theor. Chem. Acta 99 (1998) 329.
[77] J.A. Bandy, A. Berry, M.L.H. Green, R.N. Perutz, K. Prout, J.-N. Verpeaux, Chem. Commun. (1984) 729.
[78] A. Berry, M.L.H. Green, J.A. Bandy, K. Prout, J. Chem. Soc., Dalton Trans. (1991) 2185.
[79] F. Baert, J. Lamiot, L. Devos, R. Fouret, Eur. Cryst. Meet. 7 (1982) 197.
[80] C. Cambillau, G. Bram, J. Corset, C. Riche, C. Pascard-Billy, Tetrahedron 34 (1978) 2675.
[81] S. Wu, F. Gong, G. Hu, F. Miao, X. Liu, Sichuan Dax. Xuebao, Zir. Kex. (J.S. Uni. (Nat. Sci.) 25 (1988) 81.